Experiments in Fluids 25 (1998) 254–264 © Springer-Verlag 1998

Measurements of a supersonic turbulent boundary layer by focusing schlieren deflectometry

S. Garg, G. S. Settles

Abstract Some novel, non-intrusive, high-frequency, localized optical measurements of turbulence in compressible flows are described. The technique is based upon focusing schlieren optics coupled with high-speed quantitative measurement of light intensity fluctuations in the schlieren image. Measurements of density gradient fluctuations confined to a thin slice of the flowfield are thus obtained. The new instrument was used to investigate the structure of a two-dimensional, adiabatic, wind tunnel wall boundary layer at a Mach number of 3. The measurements were compared to data obtained using hot-wire anemometry and good agreement was found between the two. Distributions of broadband convection velocity of large-scale structures through the boundary later were also measured. In marked contrast to earlier results, it is shown here that the convection velocity is essentially identical to the local mean velocity. Further, results obtained using the VITA conditional sampling technique shed new light on the turbulent boundary layer structure. Overall, the data presented herein serve to validate the new measurement technique.

1 Introduction

Experimental determination of the fluctuating properties of turbulent flows is usually accomplished using either hot-wire anemometry (HWA) or laser-doppler velocimetry (LDV). These techniques have been in use for a considerable time and have undergone significant refinement since their inception. Despite this, their application to any given flow situation is often far from routine, especially for high-speed flows. In many such situations, HWA is constrained by sensor fragility, inadequate frequency response, and the disturbance of the flow by the measuring probe itself. LDV, while not requiring the insertion of probes into the flow, depends upon the presence of seed particles. For a successful measurement, these particles have to be large and numerous enough to produce a measurable signal, yet small enough to faithfully "follow" the flow and create no significant disturbance. These requirements are often difficult to satisfy in high-speed flows. In addition, the high cost of research-grade LDV systems precludes their use in laboratories of modest size and resources.

The development of alternative turbulence measuring techniques as a supplement to HWA and LDV is therefore desirable. Optical techniques, especially those not requiring flow seeding, appear particularly promising since they do not involve the insertion of probes into the flow. Further, the frequency response of photodetector-based measurement systems (both solid-state and surface-emission type) can easily be many orders of magnitude higher than that of hot-wires. Two traditional optical methods for investigating compressible flows are schlieren and shadowgraphy. Both have been widely used for qualitative flow visualization and are relatively cheap and easy to use. These techniques are sensitive to the density structure of the flow and have been used on occasion for quantitative mean density measurements. However, more interesting in the present context are the efforts to obtain quantitative turbulence data from modifications or extensions of these techniques. Some past work on this topic is reviewed below.

Kovasznay (1949) showed that, for statistically homogeneous and isotropic fluctuations, the measured spatial correlation function of shadowgraphs of turbulent flow regions could be related to the three-dimensional spectrum of the turbulent density field. Uberoi and Kovasznay (1955) provided an equivalent analysis for prediction of the spatial correlation function of the density field, from which the integral scale and the microscale of the turbulent density field could be calculated. Comparison with data gathered using HWA showed that their method worked reasonably well for the microscale but gave poor results for the integral scale—not surprising given the assumption of homogeneous, isotropic turbulence in the analysis. Thompson (1967) and Thompson and Taylor (1969) performed similar analyses with instantaneously recorded schlieren photographs of turbulent flows.

Measurement of instantaneous point values is obviously impossible using these methods. Such a measurement in a 3-D field would require the use of tomography, i.e. an optical system that employed many light rays from different directions passing through a given point. Since the majority of schlieren and shadowgraph systems use point light sources and parallel light beams, the measured quantities reflect an integral of flow

Received: *12 February 1997*/*Accepted*: *31 January 1998*

S. Garg[1], G. S. Settles
The Pennsylvania State University, University Park, PA 16802, USA

Present address:
[1]High Technology Corporation, 28 Research Drive, Hampton, VA 23666, USA

Correspondence to: S. Garg

This work was supported by NASA Grant NAG 1-1412 monitored by Dr. Leonard M. Weinstein. The VITA analysis program was adapted from one provided by Prof. Eric Spina, whose help is gratefully acknowledged.

properties along the entire path of a given ray. Only the assumptions of homogeneity and isotropy make meaningful results possible. This makes such methods unsuitable for studying the coherent, large-scale motions that play a significant role in determining the dynamics of most turbulent flows. (It should be noted that the above studies were conducted before the role of organized motions in turbulent flows was fully appreciated). Proper characterization of non-homogeneous coherent fluctuations requires techniques capable of providing "point" measurements within turbulent flows.

This requirement led to the development of some ingenious optical techniques for the study of turbulent flows. Fisher and Krause (1967) outlined a method using two mutually perpendicular light beams which intersected in the flow region of interest. The intensity of the beams was modulated by introducing water mist tracer particles in the flow, which attenuated the light beams by scattering. The cross correlation between the two resulting beam intensities after passage through the flow field was shown to yield turbulent information local to the point of beam intersection. For the particular mechanism of light extinction chosen, the results reflected the statistical properties of the fluctuating tracer particle concentration in the vicinity of the intersection point. A significant difference between this and the earlier work cited above is that it was necessary only to assume that the turbulence was "locally homogeneous" near the beam-crossing point. The technique was applied to the axisymmetric shear layer around a subsonic ($M = 0.2$) free jet which had previously been studied with the aid of HWA techniques. By separating the two light beams in the streamwise direction, measurements of the broadband convection velocity across the shear layer were obtained and found to compare favorably with hot-wire results.

Further, as pointed out by the authors, the analysis presented was sufficiently general and independent of the method employed to obtain the desired fluctuations of light intensity. Taking advantage of this fact, Wilson and Damkevala (1970) adapted the technique to use the schlieren method in a compressible turbulent flow, the results obtained then being a measure of density gradient fluctuations. With the further assumption of "local isotropy", the measured correlation between the two beams was related to the mean-square density fluctuation at the beam intersection point. Also, the spatial autocorrelation function of the density field was deduced in a manner similar to that of Uberoi and Kovasznay (1955). Davis (1971 and 1972) used a numerical technique to extract similar information from a single-beam schlieren system making use of the cylindrical symmetry of the flow field studied, an axisymmetric shear layer.

An obvious disadvantage of the techniques discussed above is that their use requires a high degree of optical access to the flow region of interest. Typically, such access is severely limited in most flow facilities not specifically designed for this purpose. This fact has prevented use of the crossed-beam correlation technique in all but free-jet/shear-layer flows.

Recently, McIntyre et al. (1991) and McIntyre (1994) devised an optical technique, dubbed "deflectometry", for the study of large-scale turbulent structures in compressible flows. The method consisted of recording the light intensity fluctuations at discrete points in a real-time schlieren image of the flowfield. Fiber optic cables in conjunction with photomultiplier tubes (PMTs) as the light detectors provided high-spatial-resolution measurements with virtually unlimited frequency response. The technique was employed to study both a low-speed CO_2/air and a high-speed ($M = 3$) air/air mixing layer. No attempt was made to relate the density gradient fluctuations to density or velocity fluctuations, as was done by earlier authors. Rather, with the assumptions that all such quantities are similarly modulated by the passage of large-scale turbulent structures, such information as the convection velocity of such structures, the power spectral density of turbulent fluctuations, and the cross-spectral density between points separated in the streamwise direction were obtained. The usual integration of fluctuations along the beam path was not an issue since the mixing layer being viewed was at the edge of a round jet. Thus, a light ray passed through a very narrow region of turbulent flow, comparable to the thickness of a single large-scale structure. The authors suggested that a more general application of this technique would only be possible with the use of sharp-focusing schlieren optics.

A possible remedy for the spatial averaging of fluctuations is the use of focusing-schlieren optics to reduce the depth-of-field of the optical system; the smaller the depth-of-focus, the closer the measurements are to "point" measurements. The first such system was described by Schardin (1942) over 50 years ago. This lens schlieren system with a large, grid-type light source was designed to provide a field of view much larger than that of mirror-type systems of similar cost. Another merit of this approach was its sharp-focusing capability, i.e. the images obtained were determined solely by density gradients in narrow "planar" region—the so-called plane of best focus. This was further demonstrated by the work of Burton (1949) and Kantrowitz and Trimpi (1950). Fish and Parnham (1950), in a review paper, pointed out several weaknesses and limitations of focusing schlieren. Two main problems cited were the difficulty of setting up and adjusting these systems and the limited fields of view which could be obtained. Other problems were low brightness and marginal quality of the image obtained. As a result, despite their potential usefulness, sharp focusing schlieren systems remained relatively undeveloped until recently.

Weinstein (1993) has recently developed a focusing schlieren system that overcomes many of the limitations of previous approaches. This system is capable of providing high-brightness, large-field images of quality comparable to that of conventional schlieren. In addition, it is capable of focusing on a near-planar region without undue loss of schlieren sensitivity. The result is a low-cost, easy-to-implement tool capable of providing schlieren images in a wide variety of flows. This focusing schlieren system was combined with the optical deflectometer of McIntyre et al. (1991) by Alvi et al. (1993) to produce a new diagnostic instrument. The technique can provide localized information on turbulent fluctuations in compressible flows. In addition, it retains the benefits of low cost, ease of use and the capability of making non-intrusive measurements.

Initial benchtop experiments undertaken with this system were relatively successful (Alvi et al. 1993). Experiments were performed with a CO_2/air mixing layer formed at the periphery of a round low-speed CO_2 jet exiting into still air. The jet was positioned such that its axis was perpendicular to the optical

axis and the top-center and bottom-center edges of the axisymmetric shear layer were in the plane of best focus. With this configuration, the Kelvin-Helmholtz vortices in the mixing layer were sharply focused and clearly visible. As the focal plane was displaced relative to the centerline of the shear layer, the images of these structures rapidly became blurred such that, at displacements of $\pm 0.2D$, they were barely visible and had completely disappeared at displacements of $\pm 0.8D$, where D is the jet diameter.

A photodetector was also used to obtain real-time, quantitative light-intensity fluctuation data for these cases. When the center plane of the jet coincided with the best focus plane, the power spectra of these fluctuations exhibited a sharp peak at a frequency corresponding to the frequency of passage of the large-scale Kelvin-Helmholtz structures. This spectral peak completely disappeared when the focal plane was displaced more than $\pm 0.2D$ from the jet centerline. Thus, the focusing ability of the instrument was demonstrated quantitatively as well as qualitatively.

Next, to broaden the range of flows examined, the authors attempted to apply the technique to a more realistic case. This was the approximately 25 mm-thick boundary layer that formed on the floor of Penn State University's supersonic wind tunnel facility. It was assumed that a 4 mm depth of focus would allow the deflectometer to focus onto one individual large-scale turbulent structure at a time. However, the first attempt failed due to inadequate schlieren sensitivity to clearly detect the density gradients in the flowfield above the background noise.

It was clear that, for successful measurement and/or visualization of this boundary layer, the optical system would require modification for much greater sensitivity. This objective was achieved via a complete re-design of the focusing schlieren component of the system. The resulting schlieren system was implemented by Bundis (1993) and proved to be a significant improvement over the original. Instantaneous, focused schlieren images of the wind-tunnel floor boundary layer were successfully obtained. In fact, the new system was sensitive enough to detect convective heat transfer from the human body to the ambient air, i.e. its sensitivity approached that of a good conventional schlieren system.

However, this improved sensitivity was achieved in part by sacrificing some sharpness of focus. Whether this precluded meaningful quantitative measurements remained to be determined. The present work aims to answer this question by applying the improved focusing schlieren apparatus, in conjunction with optical deflectometry, to obtain quantitative measurements in a supersonic turbulent boundary layer. Further, the optical data are compared to those obtained using HWA in order to validate the new technique. Finally, some comparisons are made with optical data obtained via a conventional z-type non-focusing schlieren system based on two f/8 203 mm dia. parabolic mirrors.

2
Experimental techniques

2.1
Focusing schlieren system

The focusing schlieren system employed in the present study is the lens-and-grid type described by Weinstein (1993).

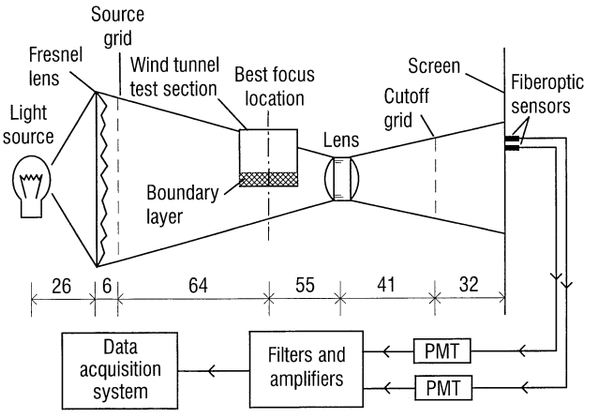

Fig. 1. Schematic diagram of the setup used for focusing schlieren measurements. The distances, in centimeters, between the various optical components are also indicated

Formulae with which to size such a system and estimate its sensitivity and depth-of-focus can be found in this reference. Since the design of such systems is discussed at length by Weinstein, only a brief description is given here. Also, relevant discussions are given by Alvi et al. (1993) and Bundis (1993).

Figure 1 is a schematic representation of the optical system used. It is based on a single, high-quality imaging lens and a source grid consisting of multiple, alternating dark bands and clear apertures in a plane. Light from an extended source is collected by a Fresnel lens, which is positioned so as to concentrate the light at the imaging lens location. This provides the maximum possible light-collection efficiency. The light back-illuminates the source grid, the multiple apertures of which act as individual schlieren sources, whereas the source grid as a whole forms the effective light source of the focusing schlieren system. This large light source produces a small depth-of-field and imparts to the multiple-source schlieren system its focusing ability.

After passage through the flow field and the imaging lens, light from the source grid is focused to form an image of the source grid in a plane optically conjugate to it. A photographic negative cutoff grid is placed in this plane. The resulting schlieren image is cast on a viewing screen placed in a plane optically conjugate to the flowfield plane of interest. Axial selectivity is achieved, in principle, by the superposition of multiple schlieren images of the object on this screen. For a given viewing screen location, images from only one plane—the ideal object plane—superimpose exactly giving a sharp, focused image. Disturbances lying outside the ideal object plane are blurred in comparison.

The deflectometer portion of the instrument consists of fiber-optic pickups embedded at points in the viewing screen that convey light intensity fluctuations via fiber-optic cables to a photodetector. The output of this photodetector is amplified, filtered, digitized and stored for subsequent analysis. Thus, the photodetector output is proportional to the density gradient in a direction perpendicular to the orientation of the source-grid lines.

The particulars of the present system are as follows: the imaging lens is an $f/3.8$, 305 mm focal length, military surplus

aerial camera lens manufactured by Pacific Optical Corp. This is by far the most expensive component of the optical system, its quality having the most direct bearing on the quality of the results obtainable. Light was provided by an ordinary 200 W soft-white light bulb powered by a variable-voltage AC transformer that allowed precise control of the illumination level. The Fresnel lens was 270 mm square and had a focal length of 215 mm. The source grid was approximately the same size as the Fresnel lens and had 0.584 mm wide clear bands separated by 3.23 mm wide dark bands, giving a source density of 2.62 lines/cm. The cutoff grid was made by photographically exposing and then developing a negative image of the source grid on high-contrast Kodalith film placed in the cutoff plane. It was about $\frac{1}{3}$ the size of the source grid. Preparation of the cutoff grid requires considerable care if good results are to be obtained, as described in greater detail below.

The distances between various components of the system are also shown on Fig. 1. These are determined using the formulae given by Weinstein (1993), taking into account the properties of the imaging lens and such factors as the desired field of view, sensitivity, depth of focus etc. Since these formulae are based on geometric optics and assume aberration-free thin lenses, they only provide starting points for setting up the system. In general, minor adjustments in the positions of the components are subsequently required to produce optimum results.

The results produced by a grid-type schlieren system also depend critically on the quality of the cutoff grid. Evenness of illumination at the cutoff grid location, sharp and uniform dark grid lines and unclouded clear grid lines are absolutely essential for good schlieren sensitivity. Careful alignment of the various components of the optical system helps ensure even illumination of the cutoff grid, and ultimately, uniformity of cutoff across the schlieren image. Imaging lens quality is the single most important determinant of the sharpness and uniformity of the cutoff grid lines. Finally, to avoid fogging of the clear grid lines, all stray light must be prevented from reaching the film during cutoff grid exposure.

The contrast between clear and dark cutoff grid lines also exerts a direct influence upon the achievable schlieren sensitivity, which is ultimately limited by the "extinction ratio" of image-plane luminance at zero cutoff to that at full cutoff. The system employed by Alvi et al. (1993) had an inadequate 6 : 1 extinction ratio, whereas the current value is about 15 : 1.

As mentioned above, this improved performance was achieved at the expense of some sharpness of focus. The depth of focus of an imaging system is inversely proportional to the maximum angle between different light rays passing through each point in the object field. Thus, an increased depth of focus of the present system over that of Alvi et al. (1993) is a direct result of the larger *f*-number of the imaging lens presently used. By a comparison of the system parameters and the formulae given by Weinstein, it is estimated that the depth of focus was approximately tripled.

The issue of depth-of-focus and its influence upon instrument performance requires careful consideration, particularly for quantitative measurements of the type proposed here. While it is true that only disturbances in the ideal object plane determine the sharp image on the viewing screen, each light beam nevertheless experiences various disturbances in traversing the flow. The final light intensity, which is determined by the total beam deflection, is therefore still dependent upon an integral of density gradients across the flow. The questions that arise are: 1) To what extent is this integration length reduced by the use of multiple-source schlieren system? and, 2) Can this integration length be related to system parameters in an objective manner?

Unfortunately, a precise definition of "depth-of-focus" is lacking, especially for present purposes. The experimental determination of system depth-of-focus, as performed by Alvi et al. (1993), provides some measure of the capabilities of a given system. However, it is important to note that their results cannot be simply extrapolated to a different flow situation, even if the optical system remains the same. This is so because the measured depth-of-focus (using their power spectrum method) is dependent on the magnitude of the density gradients being visualized. The use of a denser gas would almost certainly have resulted in a larger effective depth-of-focus.

Both Weinstein (1993) and Collicott and Salyer (1993) have attempted to define the depth of focus of multiple-source schlieren systems. The latter work presents a theoretical mutual-intensity analysis of a "*z*-type", mirror-based focusing schlieren system. Despite the differences in the specific type of system analyzed and the analysis methods themselves, the general results from the two studies are in agreement. Both define a measure that is dependent on fluid length scales as well as on the imaging system. Collicott and Salyer suggest that the outer limit of the integration length be defined as "the distance from the ideal object plane at which a disturbance in the density field has individual images completely displaced from each other". Obviously, according to this definition, disturbances of different transverse length scale will have different effective integration lengths, with smaller disturbances being integrated over a small region. Rather than relating image shift to the size of the image of the object. Weinstein (1993) chose a constant 2 mm displacement of images to define his "unsharp focus depth". He pointed out that this was an arbitrary choice, albeit one that was found to be reasonable for a variety of flows which he examined. Nevertheless, there remains an element of subjectivity in these definitions and they are thus not adopted in the present work.

Both works also indicate that the minimum depth-of-focus (termed "sharp focus depth" by Weinstein and "minimum integration length" by Collicott and Salyer) is governed by the diffractive response of the optical system. According to Weinstein, this is "the depth at which the loss of resolution due to being out of focus exceeds the resolution of the optical system and film". Collicott and Salyer developed a quantitative expression for the image-plane intensity produced by a point disturbance as a function of its distance from the ideal object plane. It is shown that this intensity drops by a factor of N within the so-called minimum integration length $(L_i)_{\min}$. Here, N is the number of sources (or gridlines) used to form the image. For a system of the present type $(L_i)_{\min}$ is given by

$$(L_i)_{\min} = \frac{4}{\alpha}\frac{\lambda d}{mb}$$

where α is the angle between light from individual gridlines, λ the central wavelength of the source light, d the distance

between the source grid and the viewing screen, b the source slit width in the plane of the cutoff grid and m is the image magnification. Weinstein's expression for the depth of sharp focus is essentially the same except that he uses the maximum beam angle (the angle between the outermost sources) rather than the angle between adjacent source beams.

Two important parameters describing the performance of a focusing schlieren system have thus been quantitatively defined. First, the maximum attenuation of an image due to being out of focus is shown to be inversely proportional to the number of gridlines. For the present system this number can be determined as follows: the optics are arranged such that the Fresnel lens forms an image of the extended light source covering the entire face of the imaging lens. Thus, each source point emits light rays at all possible angles in the direction of the viewing system. Therefore, the maximum angle between light rays passing trough a given point is determined by the imaging lens diameter and the distance from object to lens. This is 9.66° in the present case, which, when combined with a source grid-to-object distance of 63.5 cm and a source density of 2.62 lines/cm, gives $N = 28$.

Secondly, the expression for $(L_i)_{\min}$ predicts a minimum integration length of approximately 60 mm for the current system. This seems rather high and unsuitable for the study of a 25 mm-thick boundary layer. However, this distance is the object displacement that will produce an N-fold decrease in image intensity. In the present instance, with $N = 28$, this reduction in image intensity far exceeds the dynamic range of the measurement system, recalling that the extinction ratio is only about 15. From consideration of typical signal-to-noise ratios, it appears that a reduction of image intensity by as little as a factor of five is sufficient for the object to be considered effectively de-focused and "invisible". The analysis of Collicott and Salyer predicts that image intensity falls off as a sinc-squared function of object displacement, and that a fivefold decrease requires only a ± 5 mm displacement.

Due to the practical difficulties associated with achieving a depth-of-field much smaller than this, the present instrument must be considered inherently more suitable for the study of turbulent motions of this scale rather than finer-scale turbulence. It should also be noted that, even with a finite depth of focus, due to the steep drop-off of image intensity with increasing object displacement from the best-focus plane, measurements of light intensity are heavily weighted toward disturbances in the plane of best focus. Finally, note also that, if the depth-of-focus could actually be driven to zero in a practical instrument, the schlieren sensitivity would also become vanishingly small.

2.2 Experimental setup and instrumentation

The present study was performed in the supersonic wind tunnel facility of the Penn State Gas Dynamics Laboratory. For all tests, the freestream Mach number was 2.97 and the unit Reynolds number was 5.5×10^7/m. The stagnation pressure for these tests was 7.2×10^5 N/m^2 and the stagnation temperature was nominally 300 K. The tunnel walls were approximately adiabatic and the freestream turbulence level was 1–2%. The test boundary layer developed on the tunnel floor under an approximately negligible pressure gradient. Previous pitot surveys revealed that the boundary layer thickness at the test location, defined as the point where the velocity reached 99% of its freestream value, was approximately 25 mm. Integral boundary layer parameters were: $\delta = 26$ mm, $\delta^* = 7.4$ mm, $\theta = 1.7$ mm, $Re_\theta = 90000$ and $C_f = 0.0010$.

The light detectors used in the focusing schlieren deflectometer were model R928 photomultiplier tubes manufactured by Hammamatsu Optical Corp. These were powered by a 600 V source and their current output was converted to a voltage across a 1000 Ω resistance, whose value was chosen as a compromise between signal strength and frequency response. A larger resistance converts the same current into a greater voltage; on the other hand, the effective cut-off frequency of the instrument decreases with increasing resistance. It was estimated that the present cut-off frequency was well into the MHz range, thus providing more than sufficient bandwidth for the study of a turbulent supersonic boundary layer.

A TSI IFA-100 constant-temperature anemometer was used to measure the instantaneous mass flux. The hot-wire sensors were constructed by soft-soldering 5 μm diameter, platinum-plated tungsten wire onto the prongs of a TSI HWA probe. A small amount of slack was introduced into the wire to avoid strain-gaging at high frequencies. The anemometer was operated with a symmetric 1 : 1 bridge that provides much higher frequency response (up to 500 kHz) than conventional bridge settings. However, a test of the instrument's frequency response with the hot wire exposed to Mach 3 freestream airflow revealed the presence of spurious disturbances above approximately 170 kHz caused by vibration of the probe prongs. The hot-wire data were therefore low-pass-filtered at a maximum cut-off frequency of 140 kHz to avoid contamination by these fluctuations. Thus, the maximum frequency response of the hot-wire was determined not by anemometer characteristics, but rather by the mechanical construction of the probe.

The hot wires were operated at an overheat ratio approximately equal to unity. Smits et al. (1983) have shown that, at such a high overheat ratio, the hot-wire temperature sensitivity is typically much smaller than its mass flux sensitivity. With the further assumption that total temperature fluctuations are small, the temperature senstivity may be completely neglected and the hot-wire output considered to be solely a function of instantaneous mass flux.

The data acquisition system consisted of Stanford Research Systems model SRS640 filter/amplifiers for each channel and a Nicolet model 430 digital oscilloscope capable of acquiring data on two channels simultaneously at a maximum sampling rate of 10 Msamples/s. Simultaneous measurements were obtained either with two closely-spaced optical probes or with one hot wire and one optical probe, the latter positioned to sense the flow immediately upstream of the image of the hot-wire probe. The digitized data were subsequently transferred to a microcomputer for storage and analysis.

All test signals were band-pass filtered with the high pass set at 400 Hz to reduce "line" noise and low-frequency wind tunnel vibrations. The low pass was set at or below half the sampling rate to avoid aliasing errors in Fourier-spectral analysis. The actual sampling rates used depended on the particular tests being conducted: for two-point temporal correlation analysis the maximum sampling rate available was

utilized in order to provide the greatest resolution in terms of time shift. Also, no low-pass filtering was employed in these tests to avoid the temporal signal distortion that can be caused by the non-linear phase characteristics of anti-aliasing filters. For experiments in which the spectra of the fluctuating signals were of interest, lower sampling rates (typically 500 kHz) were used to provide better frequency resolution and the low-pass cut-off frequency was set appropriately.

3
Results and discussion

Fourier spectral analysis was performed on all turbulence measurements obtained. Further, the data were analyzed by using two-point space-time correlations and conditional sampling methods. The results of these analyses will now be considered in turn. In some instances, optical measurements were also taken with a conventional, non-focusing schlieren system. Where applicable, these are compared to the corresponding focusing-schlieren measurements.

It is useful at the outset to consider the quantities being measured and their relation to more commonly studied flow variables. First, since the hot-wires used in the present study were not calibrated, all hot-wire measurements are presented in terms of voltage rather than mass flux. Since the relationship between hot-wire voltage and mass flux (or velocity, in incompressible flow) is non-linear, this raises the concern that the spectra of the two quantities may not have the same shape. However, under the assumption of small perturbations, hot-wire voltage and mass flux fluctuations can be considered to be linearly related and their spectral shapes can thus be assumed to be identical.

Secondly, the quantity measured by the focusing schlieren instrument is the instantaneous first spatial derivative of the density field in a direction perpendicular to the source grid lines. Here, too, the measurements are presented in terms of the voltage output of the PMTs and no attempt is made to convert these signals to the dimensions of a density gradient. In this case however, it was independently determined that the output of the PMTs is linearly related to the light intensity (and thus to the density gradient) in the schlieren image.

3.1
Power spectra

Figure 2 shows the ensemble-averaged power spectra of optical density gradient and HWA mass flux fluctuations measured at approximately $y/\delta = 0.38$ in the test boundary layer. Curve (a) shows the spectrum of fluctuations of density gradient in the vertical direction, i.e. measured with a horizontal cutoff, whereas curve (b) shows the corresponding spectrum measured with a vertical cutoff. The spectrum of integrated density gradient fluctuations measured via conventional, horizontal-knife-edge, non-focusing schlieren is shown as curve (c). Finally, curve (d) is the spectrum of hot-wire mass flux fluctuations. The curves are plotted as a function of streamwise wavenumber, k_x, non-dimensionalized by the boundary layer thickness, δ. This wavenumber is defined as: $k_x = 2\pi/\lambda_x$, where λ_x is the x-direction wavelength of disturbances. Taylor's hypothesis of "frozen" turbulence was applied, along with the assumption that all structures move at the broadband convection velocity, to transform frequency to wavelength: $\lambda_x = U_c/f$.

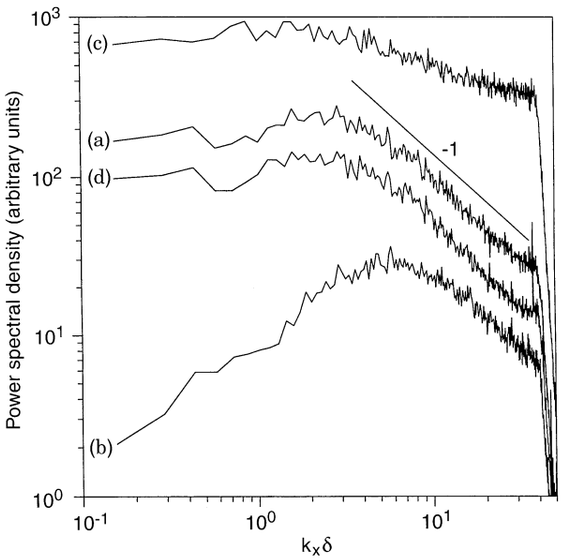

Fig. 2. Power spectra of (a) horizontal knife-edge, focusing schlieren measurements, (b) vertical knife-edge, focusing schlieren measurements, (c) horizontal-knife-edge, non-focusing schlieren measurements, and (d) hot-wire measurements

Several features of Fig. 2 deserve comment. First, it is apparent that, of the three optical data sets, only that obtained with the horizontal-knife-edge focusing schlieren system resembles the hot-wire data. Indeed, the similarity between these latter two is rather remarkable – their spectral distributions are virtually identical.

The strong Reynolds analogy (SRA) can be invoked to show that the density, velocity and mass flux fluctuations are all linearly related and thus their spectra must have the same shape. Of course, SRA requires the assumption of negligible total temperature fluctuations and pressure fluctuations much smaller than the density fluctuations. It has been shown by Bestion (1982) and Audiffren (1993) for an adiabatic flat plate boundary layer at a Mach number of 2.3 that the shapes of the spectra of mass flux and velocity fluctuations are practically the same. Note that this result does not require the most restrictive form of the SRA which assumes perfect correlation between velocity and density fluctuations, and which is not well supported by experiment (Gaviglio 1987). A milder version of the SRA, wherein the relation between density and velocity fluctuations is assumed to hold in a time-averaged sense rather than instantaneously, gives the same result. Essentially, this form of the SRA relates the r.m.s. values of density and velocity fluctuations (see Spina et al. 1991a) and has been experimentally verified by Dussauge and Gaviglio (1981).

Returning to Fig. 2, the failure of the standard, non-focusing schlieren system to provide data comparable to that obtained by a localized measuring instrument such as the hot-wire is hardly surprising. However, the strong dependence of the performance of the focusing schlieren instrument on knife edge orientation is somewhat unexpected. This behavior can be partially explained on the basis of an elementary property of the Fourier transform, which is used in estimating the power spectral density of the data. Consider the random density field

represented by $\rho(x, y, z, t)$ and its spatial derivatives $\partial\rho/\partial x$ (corresponding to a vertical knife edge) and $\partial\rho/\partial y$ (horizontal knife edge). For flow in the x-direction, the streamwise-wavenumber power spectrum is proportional to the square of the magnitude of the x-direction Fourier transform of these quantities. According to this definition, the shape of the power spectrum of ρ is unaffected by differentiation in the y-direction, whereas the spectrum of $\partial\rho/\partial x$ is k_x^2 times the spectrum of ρ. While the data shown in Fig. 2 do not strictly follow such behavior, especially at higher wavenumbers, this may also explain why the spectrum of $\partial\rho/\partial x$ increases with k_x at small wave numbers while the spectra of $\partial\rho/\partial y$ and the mass flux fluctuations are relatively constant.

Finally, both the mass flux and vertical density gradient ($\partial\rho/\partial y$) spectra exhibit a $1/k_x$ variation at moderate wavenumbers (see -1 slope indicated in Fig. 2). By considering the scaling of velocity spectra in incompressible turbulent boundary layers, Perry et al. (1986) showed that such an inverse power-law relationship is to be expected for u-velocity spectra. Smits (1995) extended this dimensional analysis to supersonic boundary layers with the same conclusions. The present data lend further support to the conclusions of these studies. Moreover, the excellent agreement between the shapes of the hot-wire and horizontal-knife-edge focusing schlieren spectra constitute validation of the localized measurement capability of the present instrument.

3.2
Streamwise correlations: convection velocity measurements

The results of a correlation analysis performed on simultaneous measurements with two optical probes separated in the streamwise (x) direction are presented in this section. The sensor separation was varied from approximately 0.25δ to 2δ at $y/\delta = 0.38$. Figure 3 shows the space-time correlation curves for the various sensor separations. The sharp peak at positive time delay ($\tau^* = \tau U_\infty/\delta$) is caused by turbulent structures convecting downstream between the measurement locations. The broadening of this peak and the reduction in its magnitude with increasing separation shows the decay of these turbulent structures. However, a significant correlation still exists for a sensor separation as large as 2δ, indicating that the structures responsible for the correlation peak are relatively long-lived.

The value of the time delay corresponding to the peak correlation can be used, along with the known separation distance between the optical probes, to compute an average, broadband convection velocity. For the range of probe separation distances tested, the resulting convection velocity is almost constant, showing a slight increase with sensor separation. This increase may be caused by the bias of the larger-separation correlations towards larger structures. Such eddies have their centers farther away from the wall and consequently tend to move faster than smaller eddies.

A profile of the broadband convection velocity was constructed by traversing the two optical probes across the boundary layer in the y-direction with a fixed Δx separation between them. This profile is shown in Fig. 4 along with the mean velocity profile; both are normalized by the free stream velocity. Also shown are the results of similar measurements with a vertical-knife-edge non-focusing schlieren system. Loss of schlieren sensitivity near the wall ($y/\delta < 0.2$) and weak

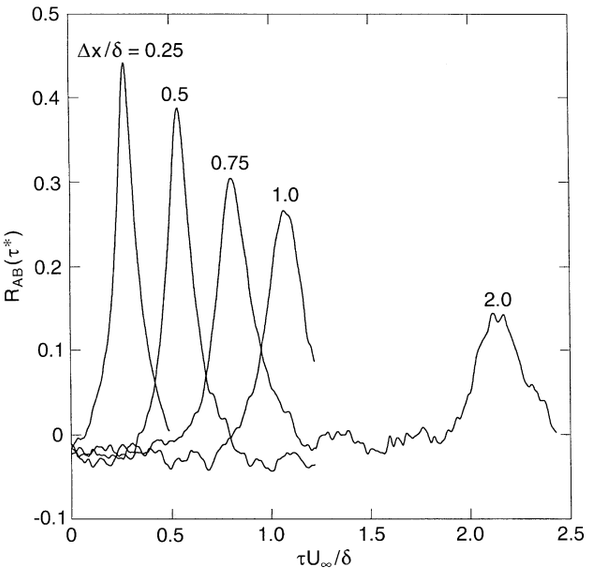

Fig. 3. Space-time correlation curves for various separations between the optical probes

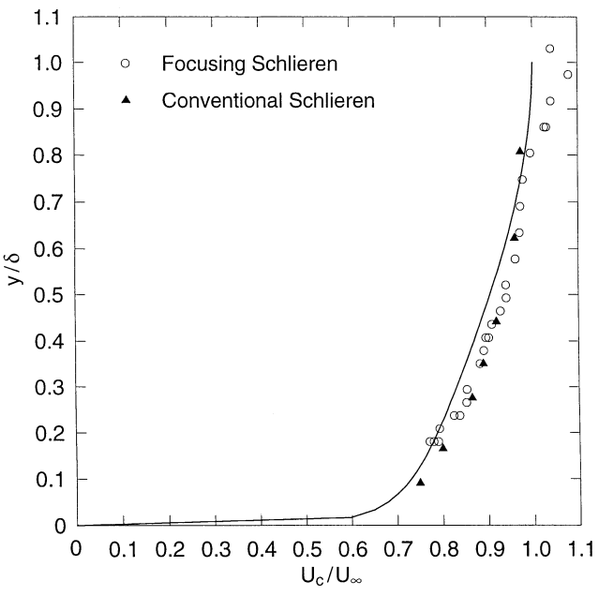

Fig. 4. Broadband convection velocity distribution through the boundary layer. The solid line is the mean velocity profile

signals near the boundary layer edge ($y/\delta > 0.8$) precluded accurate schlieren measurements in these regions.

The results presented in Fig. 4 were found to be independent of knife edge orientation. This is not surprising, since the peak time delay is based on the long-time correlation between the signals from two sensors separated by a small streamwise distance. Whatever one probe detects, so does the other, only a short time later. Thus, intuitively, knife edge orientation should have no influence on this time delay (so long as the schlieren system is actually sensitive enough to detect $\partial\rho/\partial x$ fluctuations in the absence of a mean gradient).

Also, the non-focusing schlieren system gives the same results as its focusing counterpart. This can be explained by an argument similar to the one given above: no matter what the depth of field, if there remains a signal after passage through the flow, both probes will detect it, though at slightly different times. The cross-correlation then gives the peak time delay and the convection velocity despite the contorted path that a light ray follows. The spatial integration of the conventional schlieren would thus be a drawback if the convection velocity of individual structures along the optical path varied over such a wide range that, instead of a sharp peak in the cross correlation, a wide "plateau" was obtained. In such a situation, it would not be possible to identify a single peak of the time delay. This is not the case in the present flow field. We conclude that the convection velocity of all large-scale structures across the boundary layer is about the same, thus avoiding peak broadening. In this respect, therefore, the present boundary layer is perhaps not the best flow in which to demonstrate the focusing power of the present schlieren deflectometer instrument.

The most remarkable feature of the convection velocity profile measured here and shown in Fig. 4 is that it is virtually identical to the mean velocity profile of the boundary layer (obtained by way of a pitot pressure survey and the assumptions of constant total temperature and negligible static pressure gradient across the boundary layer). This result is contrary to earlier hot-wire measurements (Owen and Horstman 1972, Spina and Smits 1987, Spina et al. 1991b), which showed an essentially constant convection velocity across the boundary layer. Note, however, that the temporal resolution of the present data is ten times better than that of the latter two studies due to the present higher sampling rate. The uncertainty in the measurements of Spina et al. could easily have hidden the variation in convection velocity observed in the present study. It is still possible that the apparent convection velocity is somehow dependent upon the instrument used to measure it, as has been remarked by earlier investigators (Spina et al. 1991b). Nevertheless, the present results indicate that the large-scale structures are fully subject to the mean shear, with their tops and bottoms moving at different speeds, rather than passively convecting downstream with their shapes intact. Also, it is apparent that the best estimate of broadband convection velocity in compressible turbulent boundary layers is simply the local mean velocity.

3.3
Vertical correlations: structure angle measurements

Space–time correlations were also obtained with two optical probes separated in the vertical direction ($\Delta y = 0.15\delta$) at various locations in the boundary layer. With the time shift applied to the lower probe, these correlations exhibited peaks at positive time delay. Since the vertically separated sensors do not lie on the same mean streamline, the peak correlation levels in this case were 2–3 times lower than those observed with a streamwise separation of sensors. Also, the peaks themselves were not always sharp and well-defined; in some instances multiple, closely spaced peaks were observed. Nonetheless, a peak was observed in all the correlations and it always occurred at a positive time delay. This implies that both sensors are detecting the same disturbance front, and that the upper sensor detects it first, i.e., the front is inclined downstream, forming an acute angle with the wall. This is entirely consistent with the conventional picture of large-scale structures in both compressible and incompressible boundary layers.

An average structure angle can be defined using the peak time delay, $\tau_{\max}$, the sensor separation, ξ, and the local convection velocity, U_c:

$$\theta = \tan^{-1}\left[\frac{\xi}{U_c \tau_{\max}}\right]$$

The previously measured convection velocity profile was used in the computation of the structure angle distribution through the boundary layer, which is shown in Fig. 5. Similar measurements have been made by Spina et al. (1991a) in a Mach 3 boundary layer using hot-wires. Their measurements indicate that the structure angle varies from approximately 40° at $y/\delta = 0.2$, to about 65° at $y/\delta = 0.8$, whereas present data fall in the range 55–72°, consistently about 10° higher than the earlier measurements. It may be that these differences can be accounted for in part by the different conditions under which the two boundary layers develop. The facility used by Spina et al. has a symmetric rectangular nozzle, whereas the present wind tunnel has a comparatively longer asymmetric rectangular nozzle. The two boundary layers were thus subjected to different pressure-gradient histories.

Another feature of Fig. 5 is the large scatter of the data. Such variance in the structure angle was also present in the hot-wire data of Spina et al. A conceivable reason for this has been mentioned above, namely: the two sensors are on different streamlines and the correlation between them is small, which causes "jitter" in the measurements. A more likely reason is that there is not a well-defined, unique angle of inclination for the large-scale structures, i.e. the disturbance front is not a straight line but rather has an irregular, convoluted shape. This causes scatter in the time delay for maximum correlation, which directly leads to scatter in the average structure angle. Therefore, the variance in these measurements should not be considered a shortcoming of the technique, but rather a characteristic of the shape of the turbulent structures themselves.

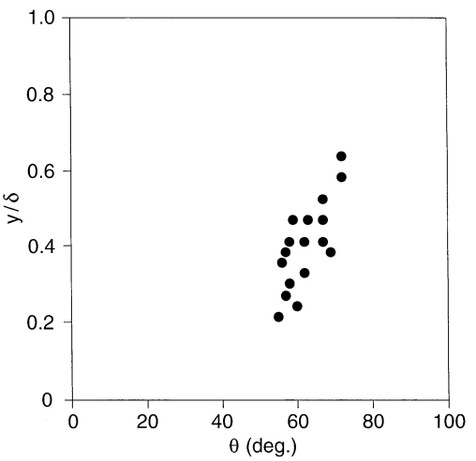

Fig. 5. Average large-scale structure angle through the boundary layer

Of course, one expects that a well-defined mean structure angle might be obtained by indefinitely increasing the averaging time. However, the data record lengths used in the present study were evidently not sufficient for this purpose.

3.4 Conditional sampling

Conditional sampling techniques were used to further demonstrate the localized measurement capability of the focusing schlieren deflectometer as well as to gain additional insight into the characteristics of organized motions in the boundary layer. These methods allow particular segments of a turbulent signal to be isolated from the rest and subsequently analyzed. The segments are chosen when they satisfy certain predetermined conditions and are said to constitute an "event". If carefully chosen, such events can be representative of typical organized motions in the turbulent flowfield. Therefore, the ensemble-averaged properties of these events can shed light on the behavior of characteristic turbulent structures.

The variable-interval time-averaging (VITA) technique of Blackwelder and Kaplan (1976) was used for conditional sampling. It has seen wide and successful use in studies of incompressible turbulent boundary layer structure. Recently, Robinson (1986), Spina and Smits (1987), and Spina et al. (1991a) have applied it to hot-wire signals in compressible boundary layers as well, finding considerable similarities between the incompressible and compressible cases. Although the application of VITA is somewhat subjective, its widespread use in turbulent boundary layer studies made it an attractive choice for present purposes. Additionally, its use allows results to be compared easily to those obtained earlier using more conventional instruments.

For details of the VITA technique the reader is referred to the original work of Blackwelder and Kaplan (1976), thus only a brief description will be given here. VITA compares the short-time-averaged variance of a fluctuating signal to its long-time-averaged counterpart. When the ratio of these quantities exceeds a preset threshold, an "event" is said to be detected. A reference point is defined for each event (usually its midpoint), and the event is classified according to the slope of the signal at this reference point. Individual positive and negative events are then separately averaged to produce the ensemble-averaged $+$VITA and $-$VITA events, respectively.

In this form, VITA detects portions of a signal where the local derivative is high, indicating the presence of a sharp gradient in the flow. Application of the technique to hot-wire signals in turbulent boundary layers has shown that the salient event is a sharp, positive, streamwise velocity gradient (or mass flux gradient in compressible flow) that extends over most of the boundary layer thickness. Such $+$VITA events are significantly more numerous and stronger than $-$VITA events. In incompressible flow, $+$VITA events have been associated with the upstream interface of large-scale turbulent structures (Chen and Blackwelder 1978). These are also called the "backs" of outer-layer structures by some investigators.

The observed characteristics of $+$VITA events in compressible boundary layers also lend support to the notion that they correspond to the upstream edges of large-scale structures (see, e.g. Spina et al. 1991a). Some additional support comes from Smith and Smits (1988, 1995), who performed simultaneous hot-wire measurements and schlieren visualizations in a Mach 3 boundary layer. Strong positive density-gradient (and hence strong positive streamwise-velocity-gradient, according to the SRA) structures were observed, with hot-wire traces similar to the $+$VITA events. However, a one-to-one correspondence could not be established due to the optical integration of the conventional schlieren system used by Smith and Smits.

If such a correspondence indeed exists, the present focusing schlieren deflectometer should be ideal for the purpose of testing the proposed connection between $+$VITA events and the upstream edges of compressible turbulent boundary layer structures. With the intention of testing this hypothesis, VITA conditional sampling was applied to simultaneously sampled hot-wire and focusing schlieren signals. The optical sensor was placed approximately 1 mm upstream of the image of the hot wire on the schlieren viewing screen (see Fig. 1). The grid was oriented vertically in this case since that provides greater fluctuating signal strength than the horizontal case. This is so because the interfaces between boundary layer and freestream fluid are, on average, inclined at an angle greater than 45° to the wall (Fig. 5), thus causing the direction of maximum instantaneous density gradient to be more nearly horizontal than vertical.

Figure 6 shows a schematic of the arrangement used for these tests, along with a model of an idealized large-scale structure. The interior of the structure contains warm, low-density/low-streamwise-momentum fluid from near the wall, whereas fluid on the outside has higher density, lower temperature, and higher momentum. Thus, the back of the structure is a sharp interface between low-density/low-momentum and high-density/high-momentum fluid, resulting in positive graidents (in the upstream direction) in both quantities across this structure. Also indicated in Fig. 6 is the direction in which light is deflected by this interface. The schlieren grid was arranged to block the source grid from the downstream direction, thus the indicated light deflection tends to cause the upstream edges of large-scale structures to appear brighter than the background in the schlieren image. In terms of PMT voltage, these structures then produce a larger negative output than the background.

The VITA technique requires the user to define two parameters: the averaging period for computation of the short-time variance, $T_{ST}^{*} = T_{ST} U_{\infty}/\delta$, and the threshold ratio of short-to-long-time variance, k, that is said to signal an event. The values of these parameters for the present study were chosen to be the same as those found to be "optimum" for the

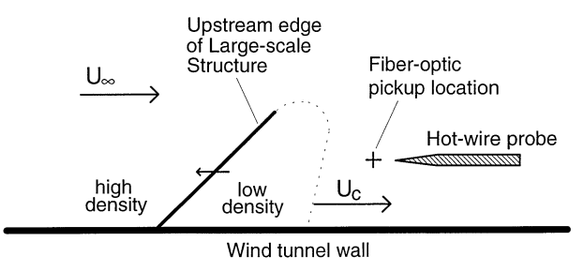

Fig. 6. Schematic representation of typical large-scale structure in the boundary layer. The direction of the density gradient detected by a vertical knife edge is indicated

detection of +VITA events by Spina and Smits (1987) in their Mach 3 boundary layer experiments: $k=0.8$ and $T^*_{ST}=0.2$. The first part of the present conditional sampling analysis was aimed at determining whether +VITA events detected by the hot-wire were also detected by the optical probe and, if so, what was the form of the ensemble-averaged schlieren signal. Event detection was thus triggered by the HWA signal and, when an event was detected, samples were collected on both the HWA and schlieren channels.

The ensemble-averaged hot-wire and schlieren events recorded at a y-location of 0.38δ are shown in Fig. 7. The average hot-wire event is very similar, both in general shape as well as in the magnitudes of the positive and negative peaks, to +VITA events detected by Spina and Smits (1987) at $y/\delta=0.43$ in their boundary layer. The typical focusing schlieren event is a negative peak which slightly precedes the hot-wire event. (Recall that the sensor in the schlieren image is positioned just upstream of the image of the hot-wire probe). Following the reasoning outlined above, this negative peak can be related to a positive density gradient in the upstream direction on the basis of schlieren grid positioning and PMT response. Thus, these observations lend strong support to the proposed connection between +VITA events and the backs of turbulent bulges in compressible flows.

Next, the conditional sampling algorithm was modified so as to detect peaks in the signals instead of sharp gradients. This can be achieved by sorting the detected events according to the sign of the signal itself rather than that of its slope. This

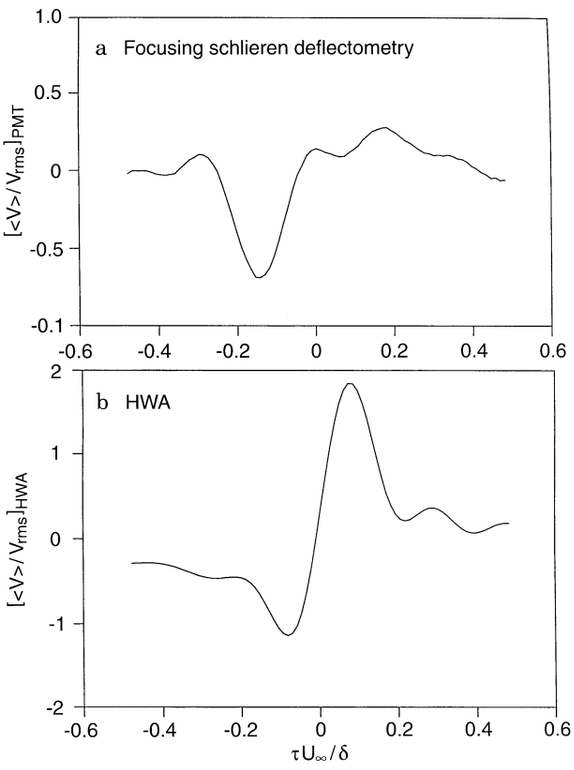

Fig. 7. Average positive VITA events detected by **a** the focusing schlieren instrument, and **b** the hot wire. Triggering is initiated by the hot-wire signal

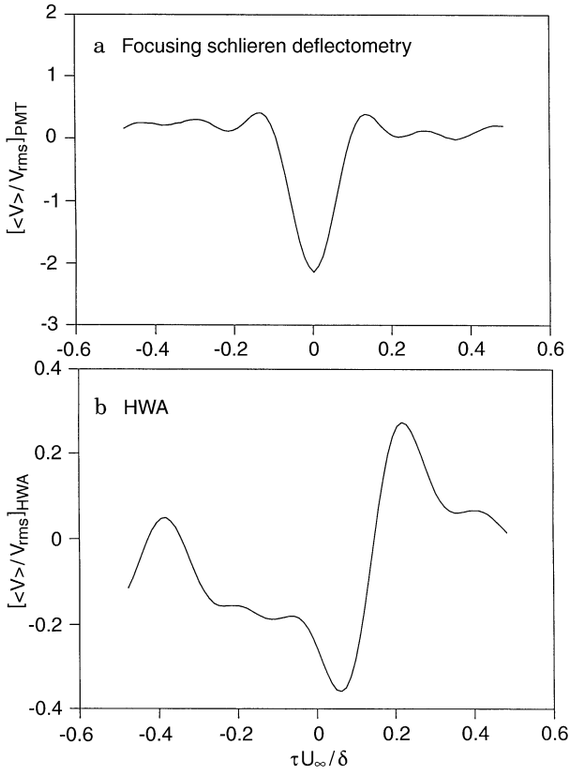

Fig. 8. Average positive VITA events detected by **a** the focusing schlieren instrument, and **b** the hot wire. Triggering is initiated by the optical signal

algorithm was applied to the schlieren signal, which was used as the triggering channel while samples were collected on both schlieren and HWA channels.

The resulting ensemble-averaged events, which are shown in Fig. 8, appear quite similar to the ones presented in Fig. 7. This lends further support to the localized measuring ability of the present instrument, since it shows that, on average, whenever the optical instrument detects an event, so does the hot wire. This would not be the case if the optical instrument were picking up events that were at other spanwise positions in the boundary layer than the local vicinity of the hot-wire.

In both Figs. 7 and 8 it can be seen that the magnitude of the peak is higher for the detecting probe event than for the other channel, regardless of whether the detecting probe is the schlieren or HWA signal. A possible explanation for this is the phase jitter between individual event detection at the triggering instrument location and its passage across the other measurement station. Also, the finite depth-of-field of the schlieren optical system likely plays a role in this phenomenon. For example, the schlieren system might detect the edges of structures narrowly missed by the hot-wire. Extending this argument it can be seen that, as the depth of field approaches infinity (as in conventional schlieren systems), there should be no correlation between events detected optically and those that appear in the hot-wire signal. Thus, the ensemble-averaged hot-wire signal should be indistinguishable from the background if the signal from a non-focusing schlieren system were used to trigger such conditional sampling. Unfortunately, this test was not included in the present test program.

4
Conclusions

This paper describes a unique optical flow diagnostic technique that is capable of making non-intrusive turbulence measurements in a wide variety of environments. Although it is primarily designed for the study of compressible flows, it could also be used in low-speed flows containing temperature or species inhomogeneities. The measurements presented and their comparison with hot-wire data serve to validate the focusing-schlieren deflectometer. Its usefulness has been demonstrated by its application to a relatively difficult situation, and by its ability to provide new insights into the behavior of compressible turbulent boundary layers. The technique has produced the most precise measurements ever made of the broadband convection velocity of large-scale structures in supersonic turbulent boundary layers. This is found to be essentially identical to the local mean velocity – a result that alters earlier notions regarding turbulent boundary layer behavior. Further evidence has been gathered to support the existence of an inverse-power-law spectral distribution of density and *u*-velocity fluctuations in turbulent boundary layers. Also, a firm connection has been established between characteristic +VITA events in the mass flux signal and the "backs" of large-scale turbulent structures.

The instrument, as described, is relatively inexpensive, easy to use and capable of extremely high frequency response. Its most expensive component is a high-quality, low-*f*-number lens. The technique described can be applied to probe three-dimensional flows where conventional optical techniques fail to provide localized, quantitative data. Another obvious advantage is that simultaneous, multi-point measurements are much easier to make than with either hot-wire or LDV techniques. Difficulties such as probe breakage and/or the necessity of properly seeding the flow are entirely avoided. Although it cannot replace conventional techniques such as HWA and LDV, focusing schlieren deflectometry can be used to supplement the data provided by these instruments. One potential drawback is that, in some flows, it might be desirable to focus to a narrower depth-of-field than is practical with this instrument.

References

Alvi FS; Settles GS; Weinstein LM (1993) A sharp-focusing schlieren optical deflectometer. AIAA paper 93-0629

Audiffren N (1993) Turbulence d'une couche limite soumise à une variation de densité due à une onde de choc ou à un chauffage pariétal. Thèse d'Universitè, Universitè d'Aix-Marseille II

Bestion D (1982) Méthodes anémomètriques par fil chaud: application à l'étude d'interactions turbulence-gradient de pression élevé en couches limites à vitesse supersonique, Thèse de Docteur-Ingénieur, Université d'Aix-Marseille II

Blackwelder RF; Kaplan RE (1976) On the wall structure of the turbulent boundary layer. J Fluid Mech 76: 89–112

Bundis EM (1993) Experiments with a sharp-focusing schlieren optical system. Senior Honors Thesis, Dept. of Mechanical Engineering, The Pennsylvania State University, University Park, PA

Burton RA (1949) A modified schlieren apparatus for large areas of field. J Opt Soc Am 39: 907–908

Chen CP; Blackwelder RF (1978) Large-scale motion in a turbulent boundary layer: a study using temperature contamination. J Fluid Mech 89: 1–31

Collicott SH; Salyer TR (1993) Noise reduction properties of a multiple-source schlieren system. AIAA paper 93-2917

Davis MR (1971) Measurements in a subsonic turbulent jet using a quantitative schlieren technique. J Fluid Mech 46: 631–656

Davis MR (1972) Quantitative schlieren measurements in a supersonic turbulent jet. J Fluid Mech 51: 435–447

Dussauge J-P; Gaviglio J (1981) Bulk dilatation effects on Reynolds stress in the rapid expansion of a turbulent boundary layer at supersonic speed. Proc 3rd Symp on Turbulent Shear Flows, University of California, Davis, 2.33

Fish RW; Parnham K (1950) Focussing schlieren systems. Aero Res Council. Tech Note No. IAP 999

Fisher MJ; Krause FR (1967) The crossed-beam correlation technique. J Fluid Mech 28: 705–717

Gaviglio J (1987) Reynolds analogies and experimental study of heat transfer in the supersonic boundary layer. Int J Heat Mass Transfer 30: 911–926

Kantrowitz A; Trimpi RL (1950) A sharp-focusing schlieren system. J Aero Sci 17: 311–314, 319

Kovasznay LSG (1949) Technique for the optical measurement of turbulence in high speed flow. Heat Transfer Fluid Mechanics Institute, American Society of Mechanical Engineers, Berkeley, CA

McIntyre SS; Stanewsky E; Settles GS (1991) An optical deflectometer for turbulence measurements. 14th ICIASF Congress, White Oak, MD, October 27–31

McIntyre SS (1994) Optical experiments and instrument development for compressible turbulent shear layers. Ph.D. Thesis, Dept. of Mechanical Engineering, The Pennsylvania State University, University Park, PA

Owen FK; Horstman CC (1972) On the structure of hypersonic turbulent boundary layers. J Fluid Mech 53: 611–636

Perry AE; Henbest S; Chong MS (1986) A theoretical and experimental study of wall turbulence. J Fluid Mech 165: 163–199

Robinson SK (1986) Space–time correlation measurements in a compressible turbulent boundary layer. AIAA paper 86-1130

Schardin (1942) Schlieren methods and their applications, Ergebnisse der Exakten Naturwissenschaften. 20: 303–309 (English translation: NASA TT F-12, 731)

Smith MW; Smits AJ (1988) Cinematic visualization of coherent density structures in a supersonic turbulent boundary layer. AIAA paper 88-0500

Smith MW; Smits AJ (1995) Visualization of the structure of supersonic turbulent boundary layers. Exp Fluids 18: 288–302

Smits AJ (1995) Mach and Reynolds number effects on turbulent boundary layer behavior. AIAA paper 95-0578

Smits AJ; Hayakawa K; Muck KC (1983) Constant temperature hot-wire anemometer practice in supersonic flows. Part 1: The normal wire. Exp Fluids 1: 83–92

Spina EF; Smits AJ (1987) Organized structures in a compressible, turbulent boundary layer. J Fluid Mech 182: 85–109

Spina EF; Donovan JF; Smits AJ (1991a) On the structure of high-Reynolds-number supersonic turbulent boundary layers. J Fluid Mech 222: 293–327

Spina EF; Donovan JF; Smits AJ (1991b) Convection velocity in supersonic turbulent boundary layers. Phys Fluids A 3: 3124–3126

Thompson JP (1967) The derivation of power spectra of density variations in hypersonic wakes from schlieren photographs. Aero Res Council C.P. No. 1021

Thompson LL; Taylor LS (1969) Analysis of turbulence by schlieren photography. AIAA J 7: 2030–2031

Uberoi MS; Kovasznay LSG (1955) Analysis of turbulent density fluctuations by the shadow method. J Appl Phys 26: 19–24

Weinstein LM (1993) Large-field high brightness focusing schlieren system. AIAA J 31: 1250–1255

Wilson LN; Damkevala RJ (1970) Statistical properties of turbulent density fluctuations. J Fluid Mech 43: 291–303